



UNIVERSITY  
OF TRENTO

---

**DIPARTIMENTO DI INGEGNERIA E SCIENZA DELL'INFORMAZIONE**

---

38123 Povo – Trento (Italy), Via Sommarive 14  
<http://www.disi.unitn.it>

SYNTHESIS OF A GALILEO AND WI-MAX THREE-BAND  
FRACTAL-ERODED PATCH ANTENNA

R. Azaro, E. Zeni, P. Rocca, and A. Massa

January 2011

Technical Report # DISI-11-058



# Synthesis of a *Galileo* and *Wi-Max* Three-Band Fractal-Eroded Patch Antenna

Renzo Azaro, Edoardo Zeni, Paolo Rocca, and Andrea Massa

Department of Information and Communication Technologies,  
University of Trento, Via Sommarive 14, I-38050 Trento - Italy

Tel. +39 0461 882057, Fax +39 0461 882093

E-mail: *andrea.massa@ing.unitn.it*,

*{renzo.azaro, edoardo.zeni, paolo.rocca}@dit.unitn.it*

Web-page: *http://www.eledia.ing.unitn.it*

# Synthesis of a *Galileo* and *Wi-Max* Three-Band Fractal-Eroded Patch Antenna

Renzo Azaro, Edoardo Zeni, Paolo Rocca, and Andrea Massa

## Abstract

In this letter, the synthesis of a three-band patch antenna working in  $E_5-L_1$  *Galileo* and *Wi - Max* frequency bands is described. The geometry of the antenna is defined by performing a Koch-like erosion in a classical rectangular patch structure according to a Particle Swarm strategy to optimize the values of the electrical parameters within given specifications. In order to assess the effectiveness of the antenna design, some results from the numerical synthesis procedure are described and a comparison between simulations and experimental measurements is reported.

## Key-words:

Antennas Synthesis, Pre-fractal Antennas, Multi-Band Antennas, Patch Antennas, Galileo/Wi-Max Bands, Particle Swarm Optimizer.

# 1 Introduction

In recent years, several researchers have devoted large efforts to develop radiating devices that satisfy the demands of the mobile telecommunication industry for improved performances in terms of multiple frequency bands and miniaturization. As a matter of fact, the design and the development of a single radiator working in two or more frequency bands is generally not an easy task especially when restrictive geometrical constraints are imposed on the radiating structure. In order to overcome the limitations of classical radiating devices (e.g., wire antennas or microstrip antennas) some investigations, both numerical and experimental, have been carried out to define alternative structures potentially able to allow improved performances [1][2][3][4]. Fractal shapes have proved to be good candidates for the development of miniaturized and multi-band antennas and several analyses have been carried out to study the radiating properties of Koch [5][6] and Sierpinski [7][8][9] shapes. Unfortunately, standard fractal or prefractal shapes show a harmonic frequency behavior instead of uncorrelated multiband resonances [5]. An effective way to face such a drawback consists in perturbing the fractal geometry by “adding” some degrees of freedom to the antenna structure. Following such an approach and avoiding the insertion of lumped loads as in [10] to obtain a multi-band behavior, some interesting results have been presented in [8] by considering a reference Sierpinski fractal shape and perturbing its scale factor. As a matter of fact, the effects of suitable perturbations on the descriptive geometrical parameters of fractals proved to be a possible way to improve their performances or modify their standard electrodynamic behavior. As an example, the optimization of geometrical parameters of pre-fractal shapes has been used to improve the radiation performances of classical fractal antennas [11]. According to such an idea, the effects of perturbations of Sierpinski-like antennas on the allocation of operating bands have been analyzed in [8]. Moreover, *Azaro et al.* showed in [12] and [13] the syntheses of non-harmonic dual-band radiators by means of the optimization of a perturbed prefractal Koch-like shape in order to comply with user-defined electrical (i.e., VSWR and gain values) and geometrical constraints.

In this letter, the multiband antenna synthesis problem is solved by considering a patch shape in order to avoid the geometrical impact of monopolar geometries and by tuning the resonance frequencies of the structure according to a Koch-like erosion process.

## 2 Three-Band Patch Antenna Synthesis

The antenna was required to operate in the  $L_1$  and  $E_5$  frequency bands of the *Galileo* positioning system ( $f_{L_1} = 1575.42 \text{ MHz}$  and  $f_{E_5} = 1191.795 \text{ MHz}$ ) and in the *Wi-Max* frequency band centered at  $f_{WM} = 2.5 \text{ GHz}$ . Moreover, a *Return Loss* lower than  $-10 \text{ dB}$  has been imposed at the input port of the antenna. Furthermore, the antenna needs of a hemispherical coverage with a main lobe width  $\theta_{-9\text{dB}} \geq 70^\circ$ . Finally, the antenna support has also been required to belong to a physical platform of dimensions  $10 \times 10 \text{ cm}^2$  above a low permittivity substrate (i.e., *Arlon* substrate with a thickness of  $h = 0.8 \text{ mm}$  and dielectric characteristics  $\epsilon_r = 3.38$  and  $tg\delta = 0.0025$  at  $f = 10 \text{ GHz}$ ).

As far as the design of the antenna geometry is concerned, a patch structure has been assumed as reference shape because of the vertical hemispherical radiation pattern suitable for both the reception of satellite signals and mobile communications [14][15]. Moreover, patch antennas are characterized by a low profile with several other advantages over other geometries [16] such as the weight, costs, and the easy integration into electronic devices (e.g., in automotive or mobile applications). In addition, recent results have shown that patch structures can be profitably modified by perturbing their original shapes to improve their geometrical and electrical performances. As an example, interesting miniaturization results have been presented in [17] and [18] where H-shaped geometries or Koch fractal shapes have been considered, respectively. Furthermore, the presence of slit cuts in the patch area has been taken into account in [19] to tune the resonance frequencies as well as to reduce the antenna dimension.

Starting from these assumptions and considerations, the design process has been recast to the erosion of perturbed Koch-like prefractal areas from a standard rectangular patch in order to tune, according to the project guidelines, multiple non-harmonic resonant frequencies. Moreover, the position of the input port has been optimized to fit with the input impedance requirements.

Accordingly and referring to a microstrip structure printed on the planar dielectric substrate, the parameters to be optimized were the perimeter of the fractal erosion along the patch sides. Following the notation in [10], the shapes of the perturbed sides of the patch antenna have been generated starting from the Koch curve and repeatedly applying the so-called Hutchinson operator. More in detail, the Hutchinson transformation has been applied only once ( $I = 1$ ) on a

side and two-times ( $I = 2$ ) on the other one to tune three non-harmonic resonant frequencies. The resulting structure turned out to be uniquely defined by determining the values of the following parameters (Fig. 1): (a) segments lengths  $L_{s,i(s),u(s),v}$ ,  $s = 1, 2$  ( $s$  being the index that identifies an eroded side of the patch),  $i(s) = 1, \dots, I(s)$  ( $i$  being the fractal stage of the  $s$ -th patch side),  $u(s) = 1, \dots, 4^{i(s)-1}$ , and  $v = 1, \dots, 4$  ( $v$  being the  $v$ -th segment of the  $u$ -th self-similar shape); (b) angles  $\Theta_{s,i(s),u(s),z}$ ,  $z = 1, 2$  ( $z$  denoting the  $z$ -angle of the  $u$ -th self-similar shape) by assuming  $\Theta_{s,i(s),u(s),1} = \Theta_{s,i(s),u(s),2}$ ; (c) coordinates  $(x_P, y_P)$  of the antenna input port (or feed point, denoted by a white dot in Fig. 1 and Fig. 2) belonging to the antenna support.

In order to fit the user-defined requirements, the values of descriptive parameters have been determined by minimizing the cost function  $\Upsilon$  proportional to the difference between requirements and estimated electrical parameters:

$$\Upsilon(\underline{\alpha}) = \min \{ \zeta(\underline{\alpha}) \} \quad (1)$$

where

$$\zeta(\underline{\alpha}) = \sum_{m=0}^{M-1} \sum_{n=0}^{N-1} \sum_{t=0}^{T-1} \left\{ \max \left[ 0, \frac{G_{\min}\{t\Delta\theta, n\Delta\phi, m\Delta f\} - \Phi\{t\Delta\theta, n\Delta\phi, m\Delta f\}}{G_{\min}\{t\Delta\theta, n\Delta\phi, m\Delta f\}} \right] \right\} + \quad (2)$$

$$+ \sum_{r=0}^{V-1} \left\{ \max \left[ 0, \frac{\Psi\{r\Delta f\} - VSWR_{max}}{VSWR_{max}} \right] \right\}$$

being  $\underline{\alpha} = \{L_{s,i(s),u(s),v}, \Theta_{s,i(s),u(s),z}; x_P; y_P; i(1) = 2; i(2) = 1; u(s) = 1, \dots, 4^{i(s)-1}; v = 1, \dots, 4; z = 1, 2\}$ .

In particular,  $\Delta f$  is the sampling step in the  $L_1$ -  $E_5$  and *Wi-Max* frequency bands,  $\Delta\theta$  and  $\Delta\phi$  are the angular steps of the gain function. Moreover,  $\Phi\{\underline{\alpha}\} = \Phi\{t\Delta\theta, n\Delta\phi, m\Delta f\}$  is the estimated gain function computed at  $(\theta = t\Delta\theta, \phi = n\Delta\phi, f = m\Delta f)$  and  $\Psi\{\underline{\alpha}\} = \Psi\{r\Delta f\}$  is the estimated *VSWR* value at the frequency  $f = r\Delta f$ .

Towards this end and according to the guidelines reported in [20][21], a suitable implementation of the *PSO* [22][23] customized to the solution of antenna synthesis problems has been integrated with a Koch-like perturbed prefractal shape generator and with a method-of-moments (*MoM*) [24] electromagnetic simulator. More in detail, a set of trial solutions  $\underline{\alpha}_p^{(k)}$  ( $p = 1, \dots, P$ , being the trial solution index) has been iteratively ( $k$  being the iteration index) defined by means of the *PSO* strategy and evaluated by computing the corresponding cost values  $\Upsilon_p^{(k)} = \Upsilon(\underline{\alpha}_p^{(k)})$  until  $k = K$  or  $\Upsilon_{opt}^{(k=k_{conv})} \leq \eta$ ,  $\eta$  being the convergence threshold and

$\Upsilon_{opt}^{(k)} = \min_k \{ \Upsilon^{(k)} \}$  where  $\Upsilon^{(k)} = \min_p \{ \Upsilon_p^{(k)} \}$ . As far as the computation of the cost values are concerned, both *Return Loss* and gain values have been computed by means of the *MoM* simulator, which takes into account the presence of the substrate as well as of the reference ground plane assumed of infinite extent.

### 3 Numerical Simulation and Experimental Validation

In order to synthesize the three-band antenna, the following setup for the *PSO*-based optimization procedure has been assumed: a dimension of the swarm equal to  $P = 8$ , the convergence threshold fixed to  $\eta = 10^{-3}$ , and a maximum amount of iterations equal to  $K = 200$ .

For illustrative purposes, Figures 2 and 3 show the evolution of the optimal trial solution,  $\underline{\alpha}_{opt}^{(k)}$ , and the corresponding *Return Loss* behavior during the minimization process, respectively. As it can be noticed (Fig. 2), the geometrical parameters of the fractal boundary are mainly varied during the first iterations [Figs. 2(a)(b)], while the location of the feed point is modified throughout the whole process [Figs. 2(a)-(e)] for a precise tuning and matching of the antenna with minor modification to the fractal perimeter when  $k > 10$ . Accordingly (see Fig. 3), starting from a very poor solution [Fig. 2(a) -  $k = 0$ ] the optimization process is able to determine better and better geometries until the final structure [Fig. 2(e) -  $k = k_{conv}$ , being  $k_{conv} = 103$ ] fully fits the requirements both in terms of electrical (Fig. 3 - *VSWR*; Fig. 4 - Horizontal gain values; Fig. 5 - Vertical gain values) and geometrical parameters (78 [mm] along the  $x$ -axis and 61 [mm] along the  $y$ -axis with the feed point located at  $x_P = 3.2$  mm and  $y_P = 4.2$  mm). As far as the radiation properties are concerned, the designed antenna allows a hemispherical coverage as expected when dealing with patch-like structures and further confirmed by both numerical and experimental results shown in [17] [18] [19].

For completeness, the behavior of the optimal value of the cost function,  $\Upsilon_{opt}^{(k)}$ , versus the iteration number  $k$  is shown in Fig. 6. Concerning the computational burden, each *PSO* iteration took a *CPU*-time of about 30 sec on a Pentium IV 1800 MHz with 512 MB RAM memory.

In order to perform an experimental validation, a prototype of the synthesized antenna has been fabricated (Fig. 7) and measured. During the measurements, the prototype has been equipped with an *SMA* connector and placed on a reference finite ground plane with dimensions of  $90 \times 140$  cm<sup>2</sup>. The *Return Loss* values have been measured with a scalar network analyzer



in a controlled environment and the results are compared with numerical data in Fig. 8. As it can be observed, although an satisfactory agreement has been achieved, there are some differences between numerical and experimental results (especially in the Wi-Max band) probably due to the following motivations: (a) the electromagnetic model of the dielectric substrate is more carefully approximated at the lower frequencies and the model accuracy reduces at higher frequencies; (b) unlike simulations, the measurement ground plane is of finite extent and finite conductivity.

Concerning the bandwidth issue, the  $L_1$  and  $E_5$  Galileo signals present narrow spectra (approximately of about  $10 \div 20 MHz$ ) and the resonance bands of the synthesized antenna meet such a requirement. The same conclusion holds true for the Wi-Max band, as well, since a sufficient bandwidth (of approximately  $30 MHz$ ) has been obtained to allocate a finite set of Wi-Max channels.

## 4 Conclusions

The design of a three-band patch antenna working in  $E_5$ - $L_1$  Galileo and *Wi - Max* frequency bands has been presented. The synthesis problem has been reformulated in terms of an optimization one by considering a reference patch antenna and successive perturbations according to fractal-shaped erosion in order to tune the resonance frequencies. A prototype of the antenna has been built and some comparisons between measured and simulated *Return Loss* values have been carried out to demonstrate the effectiveness and reliability of the synthesis process.

## Acknowledgements

This work has been supported in Italy by the “Progettazione di un Livello Fisico ‘Intelligente’ per Reti Mobili ad Elevata Riconfigurabilità,” Progetto di Ricerca di Interesse Nazionale - MIUR Project COFIN 2005099984.

## References

- [1] D. H. Werner and R. Mittra, *Frontiers in electromagnetics*. Piscataway: IEEE Press, 2000.
- [2] J. Gianvittorio and Y. Rahmat-Samii, "Fractals antennas: A novel antenna miniaturization technique, and applications," *IEEE Antennas Propagat. Mag.*, vol. 44, pp. 20-36, Feb. 2002.
- [3] S. R. Best, "A comparison of the resonant properties of small space-filling fractal antennas," *IEEE Antennas Wireless Propag. Lett.*, vol. 2, pp. 197-200, 2003.
- [4] J. M. Gonzàles-Arbesù, S. Blanch, J. Romeu, "Are space-filling curves efficient small antennas?," *IEEE Antennas Wireless Propag. Lett.*, vol. 2, pp. 147-150, 2003.
- [5] C. P. Baliarda, J. Romeu, and A. Cardama, "The Koch monopole: a small fractal antenna," *IEEE Antennas Propagat. Mag.*, vol. 48, pp. 1773-1781, Nov. 2000.
- [6] S. R. Best, "On the performance properties of the Koch fractal and other bent wire monopoles," *IEEE Trans. Antennas Propagat.*, vol. 51, pp. 1292-1300, Jun. 2003.
- [7] Puente, J. Romeu, R. Pous, X. Garcia, and F. Benitez, "Fractal multiband antenna based on the Sierpinski gasket," *Electron. Lett.*, vol. 32, pp. 1-2, Jan. 1996.
- [8] C. Puente, J. Romeu, R. Bartoleme, and R. Pous, "Perturbation of the Sierpinski antenna to allocate operating bands," *Electron. Lett.*, vol. 32, pp. 2186-2188, Nov. 1996.
- [9] C. Puente, J. Romeu, R. Pous, and A. Cardama, "On the behavior of the Sierpinski multi-band fractal antenna," *IEEE Trans. Antennas Propag.*, vol. 46, pp. 517-524, Apr. 1998.
- [10] D. H. Werner, P. L. Werner, and K. H. Church, "Genetically engineered multiband fractal antennas," *Electron. Lett.*, vol. 37, pp. 1150-1151, Sep. 2001.
- [11] M. Fernandez Pantoja, F. Garcia Ruiz, A. Rubio Bretones, S. Gonzales Garcia, R. Gomez Martin, J. M. Gonzales-Arbesù, J. Romeu, J. M. Rius, P. L. Werner, and D. H. Werner, "GA design of small thin-wire antennas: comparison with Sierpinski type prefactal antennas," *IEEE Trans. Antennas Propag.*, vol. 54, pp. 1879-1882, Jun. 2006.

- [12] R. Azaro, G. Boato, M. Donelli, A. Massa, and E. Zeni, "Design of a prefractal monopolar antenna for 3.4-3.6 GHz Wi-Max band portable devices," *IEEE Antennas Wireless Propag. Lett.*, vol. 5, pp. 116-119, 2006.
- [13] R. Azaro, F. De Natale, M. Donelli, E. Zeni, and A. Massa, "Synthesis of a prefractal dual-band monopolar antenna for GPS applications," *IEEE Antennas Wireless Propag. Lett.*, vol. 5, pp. 361-364, 2006.
- [14] R. Garg, P. Bhartia, I. Bahl, and A. Ittipiboon, *Microstrip Antenna Design Handbook*. Norwood, MA: Artech House, 2001.
- [15] D. M. Pozar and D. H. Schaubert, *Microstrip Antennas: the Analysis and Design of Microstrip Antennas and Arrays*. New York, NY: IEEE Press, 1995.
- [16] N. Padros, J. I. Ortigosa, J. Backer, and M. F. Iskander, "Comparative study of high-performance GPS receiving antenna designs," *IEEE Trans. Antennas Propag.*, vol. 45, pp. 698-706, Apr. 1997.
- [17] D. Singh, P. Gardner, and P.S. Hall, "Miniaturised microstrip antenna for MMIC applications," *Electron. Lett.*, vol. 33, pp. 1830-1831, Oct. 1997.
- [18] J. Guterman, A. A. Moreira, and C. Peixeiro, "Dual-band miniaturized microstrip fractal antenna for a small GSM1800 + UMTS mobile handset," in *Proc. IEEE MELECON 2004*, Dubrovnic, Croatia, May 12-15, 2004
- [19] X. Zhang, and F. Yang, "Study of a slit cut on a microstrip antenna and its applications," *Microw. Opt. Technol. Lett.*, vol. 18, no. 4, pp. 297-300, Jul. 1998.
- [20] J. Kennedy, R. C. Eberhart, and Y. Shi, *Swarm Intelligence*. San Francisco: Morgan Kaufmann Publishers, 2001.
- [21] J. Robinson and Y. Rahmat-Samii, "Particle swarm optimization in electromagnetics," *IEEE Trans. Antennas Propagat.*, vol. 52, no. 2, pp. 397-407, Feb. 2004.
- [22] M. Donelli and A. Massa, "A computational approach based on a particle swarm optimizer for microwave imaging of two-dimensional dielectric scatterers," *IEEE Trans. Microwave Theory Techn.*, vol. 53, no. 5, pp. 1761-1776, May 2005.

- [23] R. Azaro, F. De Natale, M. Donelli, A. Massa, and E. Zeni, "Optimized design of a multi-function/multi-band antenna for automotive rescue systems," *IEEE Trans. Antennas Propagat.*, vol. 54, no. 2, pp. 392-400, Feb. 2006.
- [24] R. F. Harrington, *Field Computation by Moment Methods*. Malabar, Florida: Robert E. Krieger Publishing Co., 1987.

## Figure Captions

- **Figure 1.** Descriptive parameters.
- **Figure 2.** Geometrical structure of the patch antenna at different iterations of the optimization process: (a)  $k = 0$ , (b)  $k = 10$ , (c)  $k = 50$ , (d)  $k = 80$ , and (e)  $k = k_{conv}$ .
- **Figure 3.** Behavior of the *Return Loss* values at the input port of the patch antenna at different iterations of the optimization process.
- **Figure 4.** Behavior of the simulated gain function in the horizontal plane [ $\theta = 90^\circ$ ].
- **Figure 5.** Behavior of the simulated gain function in the vertical planes [(a) -  $\phi = 0^\circ$ , (b) -  $\phi = 90^\circ$ ].
- **Figure 6.** Behavior of the optimal value of the cost function,  $\Upsilon_{opt}^{(k)}$ , versus the iteration number  $k$ .
- **Figure 7.** Photograph of the prototype of the three-band patch antenna.
- **Figure 8.** Comparison between measured and simulated *Return Loss* amplitude values.

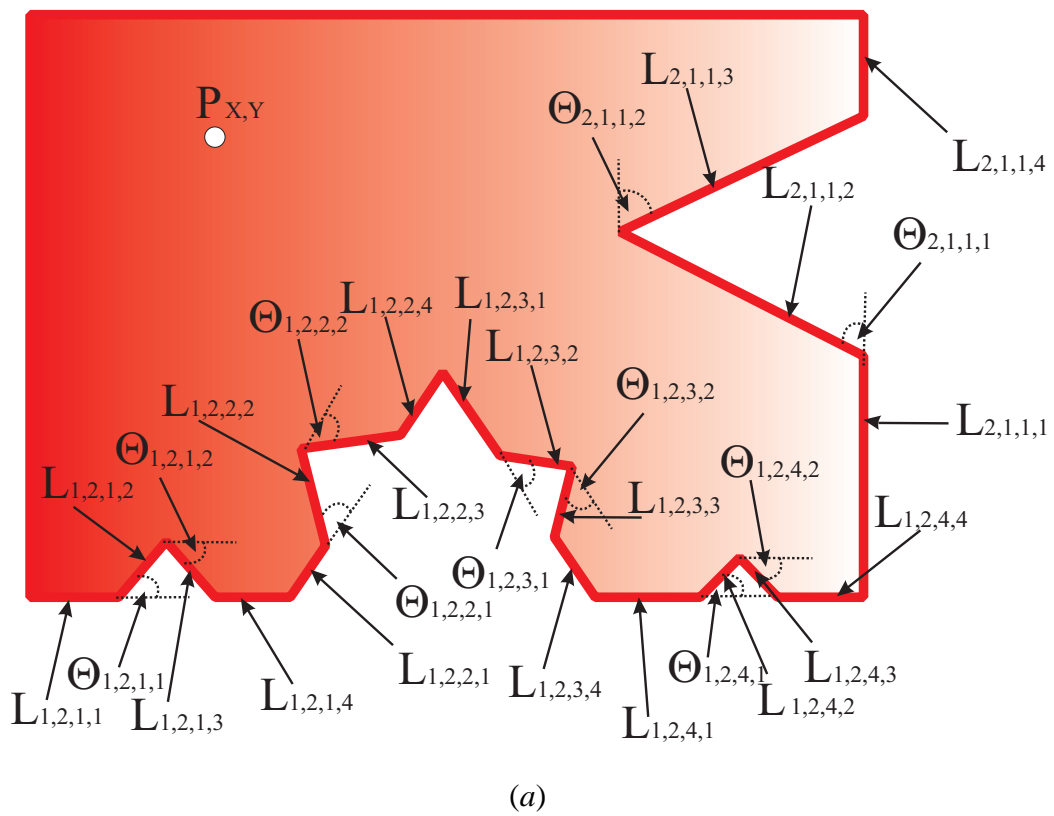


**Fig. 1 - R. Azaro et al., “Synthesis of a Galileo and Wi-Max three-band ...”**

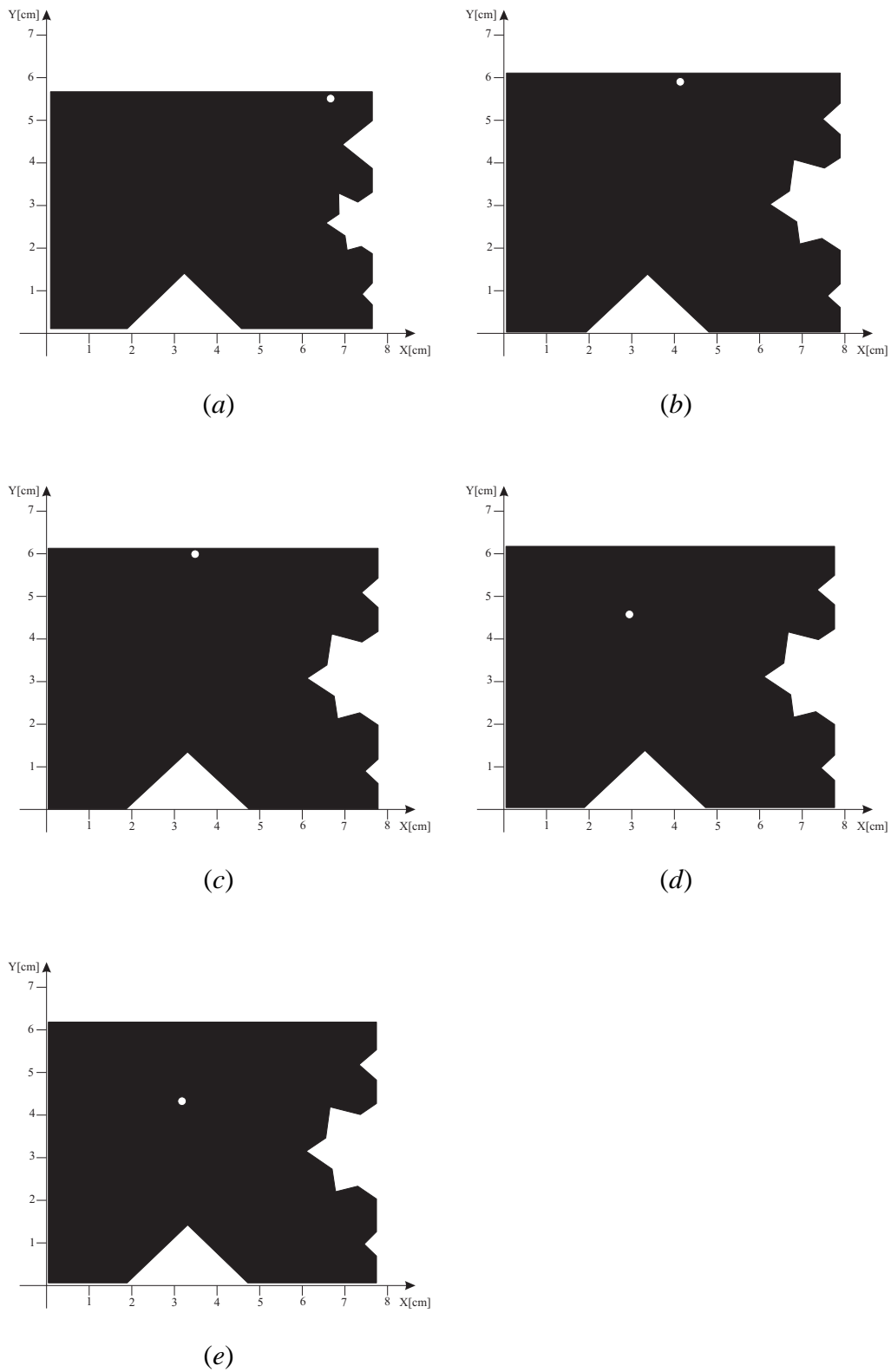


Fig. 2 - R. Azaro *et al.*, “Synthesis of a *Galileo* and *Wi-Max* three-band ...”

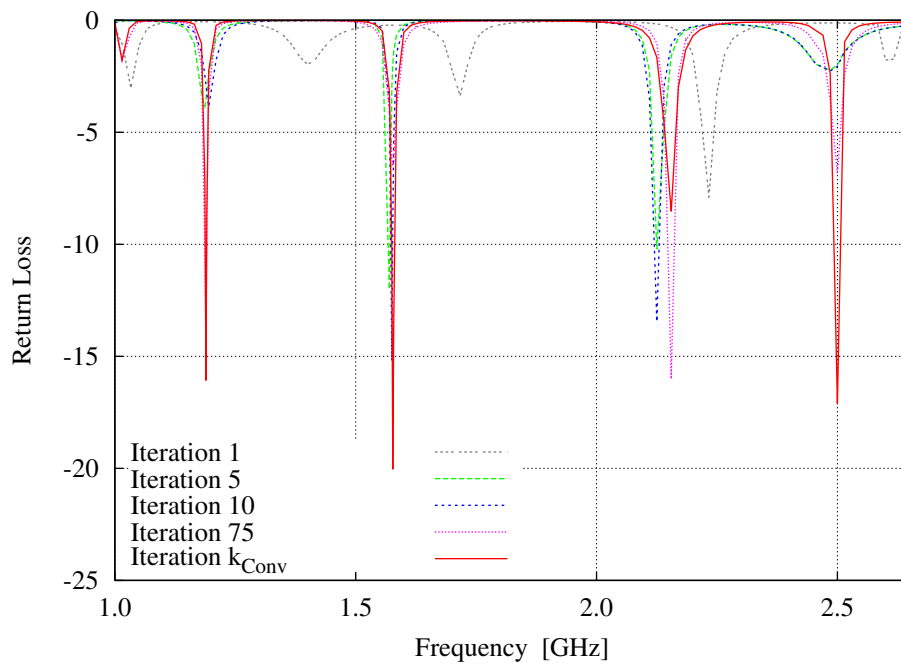


Fig. 3 - R. Azaro *et al.*, “Synthesis of a *Galileo* and *Wi-Max* three-band ...“



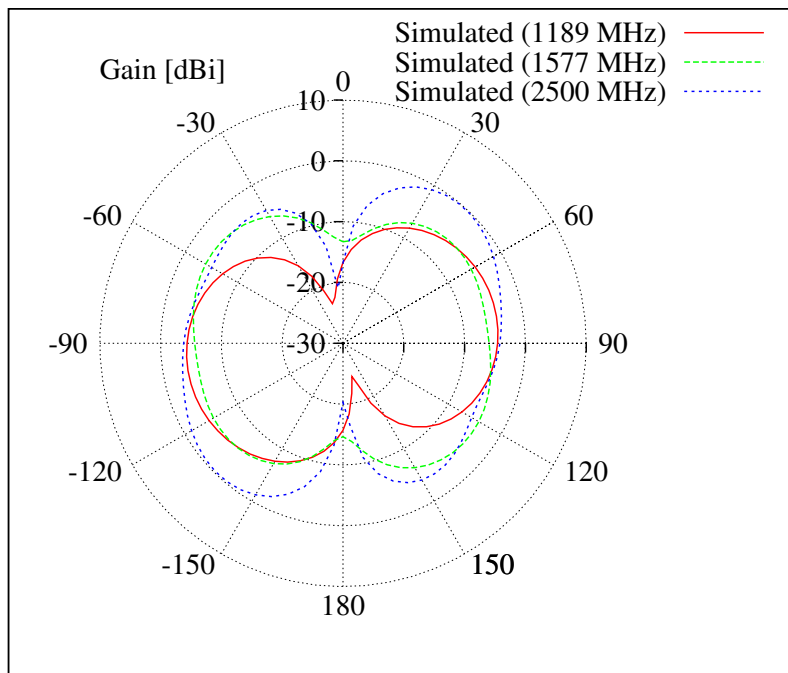
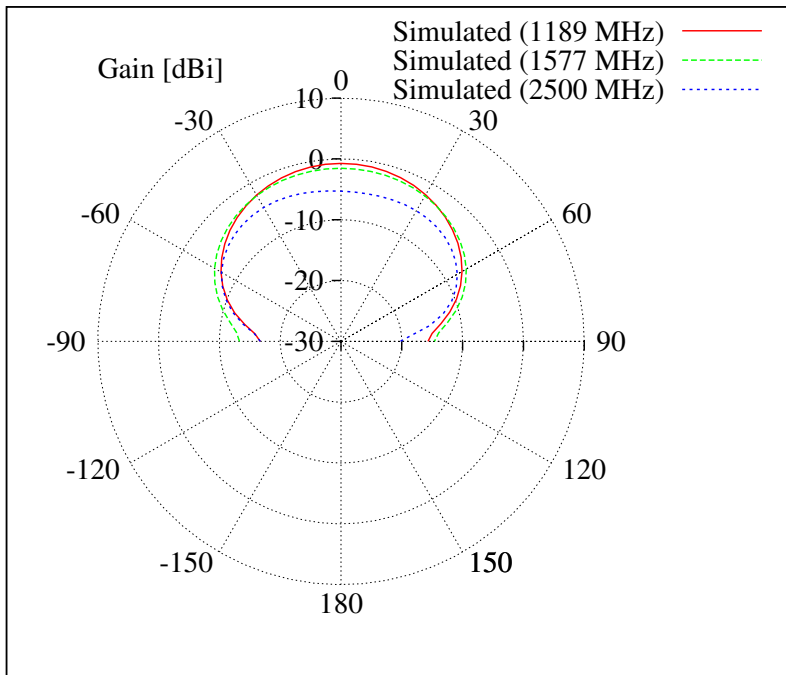
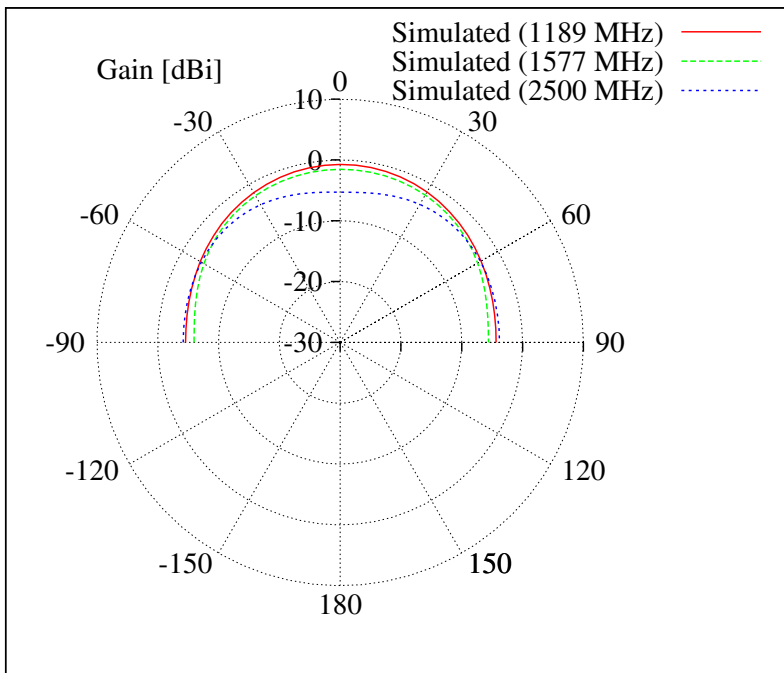


Fig. 4 - R. Azaro *et al.*, “Synthesis of a *Galileo* and *Wi-Max* three-band ...“



(a)



(b)

Fig. 5 - R. Azaro *et al.*, “Synthesis of a *Galileo* and *Wi-Max* three-band ...”

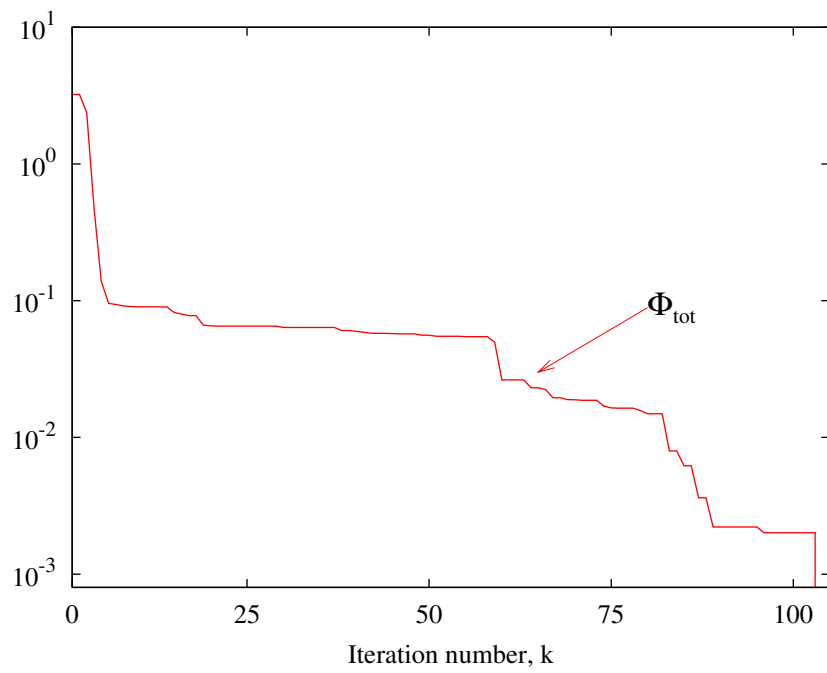


**Fig. 6 - R. Azaro *et al.*, “Synthesis of a Galileo and Wi-Max three-band ...”**



**Fig. 7 - R. Azaro *et al.*, “Synthesis of a *Galileo* and *Wi-Max* three-band ...“**

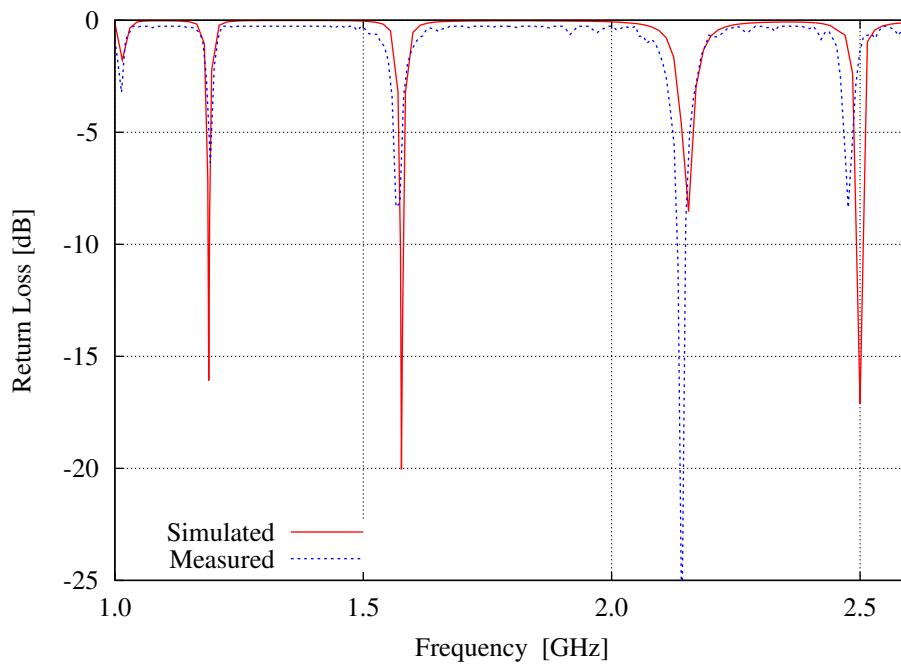


Fig. 8 - R. Azaro *et al.*, “Synthesis of a *Galileo* and *Wi-Max* three-band ...“